JTTEE5 17:254–262
DOI: 10.1007/s11666-008-9167-3
1059-9630/$19.00 © ASM International

Study of the HVOF Ni-Based Coatings' Corrosion Resistance Applied on Municipal Solid-Waste Incinerators

J.M. Guilemany, M. Torrell, and J.R. Miguel

(Submitted May 11, 2007; in revised form September 6, 2007)

Oxidation of exchanger steel tubes causes important problems in Municipal Solid-Waste Incinerator (MSWI) plants. The present paper shows a possible solution for this problem through High-Velocity Oxygen Fuel (HVOF) thermal spray coatings. A comparative study was carried out between powder and wire Ni-based thermal spray coatings (with the same composition). These optimized coatings were compared based on their microstructure, wear properties (ASTM G99-90, ASTM G65-91), and erosion-corrosion (E-C) resistance. An E-C test designed in the Thermal Spray Centre was performed to reproduce the mechanisms that take place in a boiler. Studying the results of this test, the wire HVT Inconel coating sprayed by propylene appears to be the best alternative. A commercial bulk material with a composition similar to Ni-based coatings was tested to find the products of the oxidation reactions. The protective mechanisms of these materials were assessed after studying the results obtained for HVOF coatings and the bulk material where the presence of nickel and chromium oxides as a corrosion product can be seen. Kinetic evolution of the Ni-based coatings can be studied by thermogravimetric analysis. The protection that Inconel coatings give to the tube through the difference of the gain mass can be seen. Ni-based HVOF coatings by both spray conditions are a promising alternative to MSWI protection against chlorine environments, and their structures have a very important role.

Keywords coating, corrosion, erosion, HVOF, Ni based, oxidation, waste

1. Introduction

Degradation problems in the municipal solid-waste incinerator require technological solutions. Thermal spray coatings can improve the E-C resistance of these plants, and the HVOF coatings of Ni-based alloys are a good solution. HVOF coatings give compact, low porosity, homogeneous, and hard structures with enough thickness to stop the advancing of electrolytes (Ref 1-5).

Temperatures in the exchanger zone are about 760 °C. At these temperatures, some of the most important corrosive agents are chloride salt mixtures. Concretely, KCl:$ZnCl_2$ eutectic mixtures are very corrosive due to their low melting point (Ref 2, 6-9).

Such mixtures and other compounds, such as NaCl, K_2SO_4, cause damage to tubes (Ref 9). The molten mixture of salts impacts on the tubes' surfaces. After this impact and due to their melted morphology, the mixture remains stuck, thus starting the corrosion process. The present paper compares wire and powder thermal spray coatings of the same Ni alloy. Wire and powder alloy was sprayed by different guns, in different conditions using different combustion gas, mixtures. The target has been to determine the role of the material composition and coating structure in the MSWI superheaters protection through different sides of the HVOF thermal spray technology. Tribological and microhardness characterization of the coatings was done.

Erosion and corrosion resistance were evaluated through designed laboratory tests using a KCl:$ZnCl_2$ eutectic mixture as a corrosion agent. The thickness difference after 12 h under testing conditions was used to compare the resistance of both coatings. In situ tests on coatings and laboratory tests on bulk Ni alloys were also made to understand the mechanisms of protection of these Ni alloy coatings. Results of these tests were evaluated by SEM images and EDS analysis as well as XRD.

J.M. Guilemany, M. Torrell, and **J.R. Miguel**, Thermal Spray Centre (CPT), University of Barcelona, Barcelona, Spain. Contact e-mail: mtorrell@ub.edu.

2. Experimental Method

2.1 Materials Coatings

Tested coatings were obtained using an HVT gun for the wire coating and a DJH 2600 for the powder coating. Material composition is detailed in Table 1. The steel used as a substrate was an AISI C-1055 (UNS G10550).

Substrates were cleaned with acetone in an ultrasound bath before spraying and grit-blasted with corundum at 5.6 bar to have a roughness of $R_a \geq 5$ μm. Spraying conditions of both coatings are detailed in Table 2.

Propylene (C_3H_6) was used as a combustion gas in sprayed wire and hydrogen for the spray used in the powder coatings. The stoichiometry (O_2/H_2) of the flame was 0.48 for the powder coating and 2.7 (O_2/C_3H_6) for the wire coating. Samples were sprayed in a cool environment, minimizing the oxide production. The coating oxidations during the spray process decrease their corrosion resistance under chloride agents. On the other hand, interconnected porosity must be avoided.

Bulk materials with similar composition of coatings were tested by static corrosion test. The composition of bulk material is detailed in Table 3.

Table 1 Composition of the feedstock material

Feedstock		Ni	Fe	Cr	Mo	Al	Nb	Ti
A-625	Wire	Bal	5	21.2	8.3	0.5	1.2	0.01
B-625	Powder							

Table 2 Spraying conditions

	Fuel, psi	Flame stoichiometry	Distance, mm
A-625	75 (C_3H_6)	2.7	125
B-625	635 (H_2)	0.48	250

Table 3 Composition of bulk material

	Ni	Cr	Fe	Mo	Nb	Co	Si	Mn	Al	Ti
B1	Bal	20-23	5	8-10	3.5	1	0.5	0.5	0.4	0.4

2.2 Characterization Techniques

Tribological properties of these coatings were characterized by two standardized wear tests, one to evaluate friction wear resistance (Ball-on-Disk ASTM G99-90), the other to evaluate abrasive wear resistance (Rubber-Wheel ASTM G65-91 D).

The Ball-on-Disk test was done at 25 °C with relative moisture below 20%, and using WC-Co balls as counterparts. 0.11 m/s was the lineal sliding speed and 1000 m was the accumulated sliding distance. The applied load was 5 N.

The Rubber-wheel text applied a load of 50 N, a silica flow of 295 ± 2 g/min, and a rubber wheel velocity of 139 rpm.

Vickers microhardnesses were measured using a Matsuzawa MX T-α, and 20 measurements for each coating were done to find their microhardness on cross section (ASTM E 384-99).

The E-C device is a blowpipe of hot air that expels air at 650 °C, and this flow is used to propel onto the substrate a drop of the aqueous solution 0.05 M of a eutectic mixture KCl:$ZnCl_2$ (52:48 wt.%) (Ref 10). The air is hot enough to evaporate the water of the solution, keeping the molten salt on the surface of the sample that is above 450 °C as the reported superheater tube surface (Ref 11). This device simulates the flue gas impacting on the tubes. The test runs for 12 h, spraying 1 L of salt solution. The device scheme is detailed in Fig. 1. The post-test evaluation is done by comparing the loss of thickness of the coatings. The analysis of the possible phases was made using Scanning Electron Microscopy (SEM) JEOL 5310 with a Röntec Energy Dispersive Spectroscopy (EDS) analyzer. Polished cross sections of the samples were dry prepared to avoid the dissolution of the possible phases created by corrosion mechanisms (Ref 12).

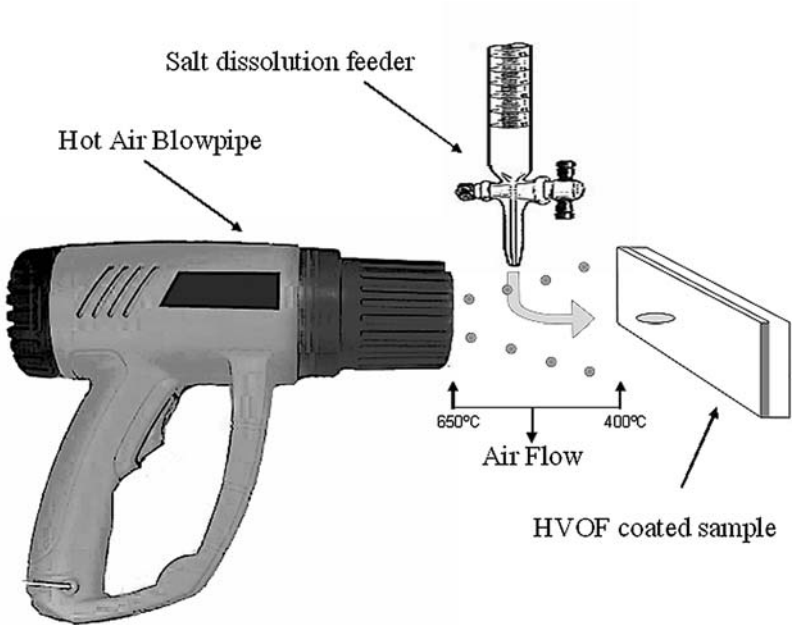

Fig. 1 Scheme of the E-C device

The loss of thickness is due to a combination of the erosion process caused by the impact of the hot air and salts and the oxidation of the molten salts. The corrosion processes are more aggressive than the erosion process. Therefore, composition and corrosion resistance of the used materials are more important than coating mechanical properties.

2.3 In Situ Test

Exchanger tubes were coated with the Ni alloy and welded inside the incinerator boiler. These tubes were welded in the first set of the superheaters and left in service for 1 year and then cut and examined. Cross sections were prepared and studied. This test was used to compare the reproducibility of the E-C test designed in the CPT laboratory. Stereoscopic microscopy was also used for a first evaluation of the pipes' surface. The coatings' loss of thickness was evaluated by SEM images. Maps of the concentration of elements were obtained by EDS. Coated and uncoated steel tube samples were tested using a thermogravimetric test by a Scanning Differential Thermogravimetric analyzer SDT 2960 (TA instruments, New Castle, Delaware, USA). After a drying step, the samples were tested for 120 h at 400° covered by a $KCl:ZnCl_2$ salt mixture.

2.4 Static Corrosion Test on Bulk Material

A static corrosion test was made for the bulk material with a similar composition of a Ni-based alloy previously used for the E-C and in situ tests.

Samples with 2 cm^2 of surface were covered with an excess of eutectic salt mixture and tested for 360 h at 400 °C. Results were evaluated through XRD and EDS analyses to characterize the produced corrosion phases.

3. Results and Discussion

3.1 Material Structure

X-ray diffraction of the feedstock materials (wire and powder) shows the same Ni-Fe solid solution structure as can be seen in Fig. 2.

Structures of both coatings as sprayed are shown in Fig. 3(a) and (b), where a homogeneous coat is observed. The wire coating sprayed by HVT (C_3H_6) in Fig. 3(a) shows a compact and thicker structure with more oxidation than powder coating sprayed by DJH (H_2). The spray oxidation product that was found was Cr_2O_3 on the splat

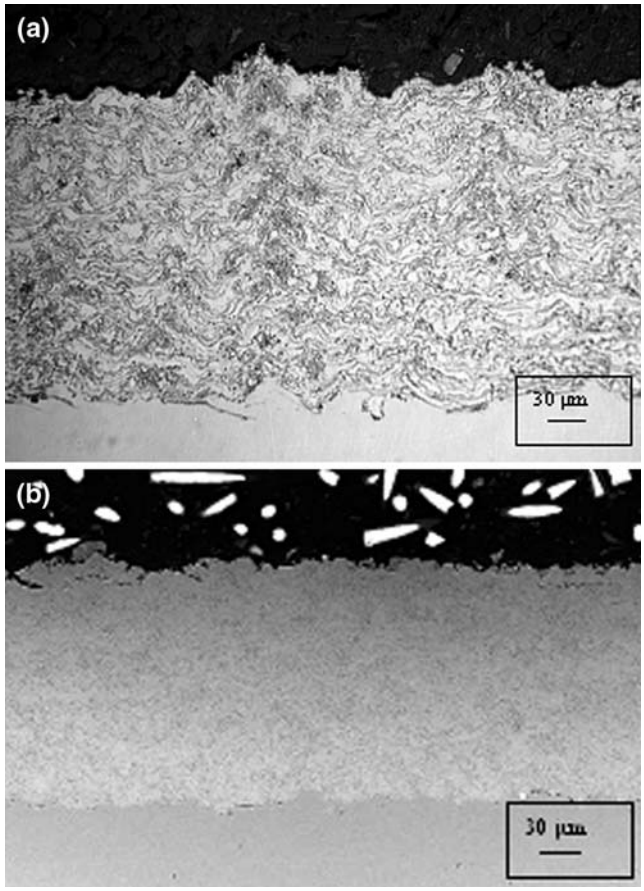

Fig. 3 (a) SEM structure of A-625 and (b) SEM structure of B-625

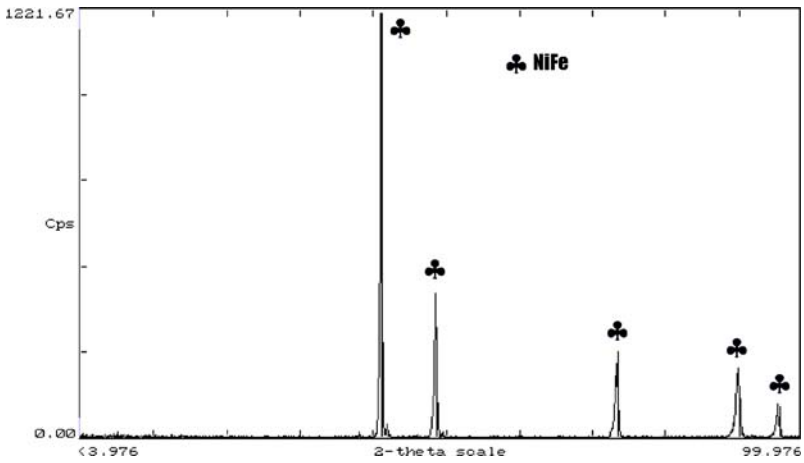

Fig. 2 XRD of feedstock materials

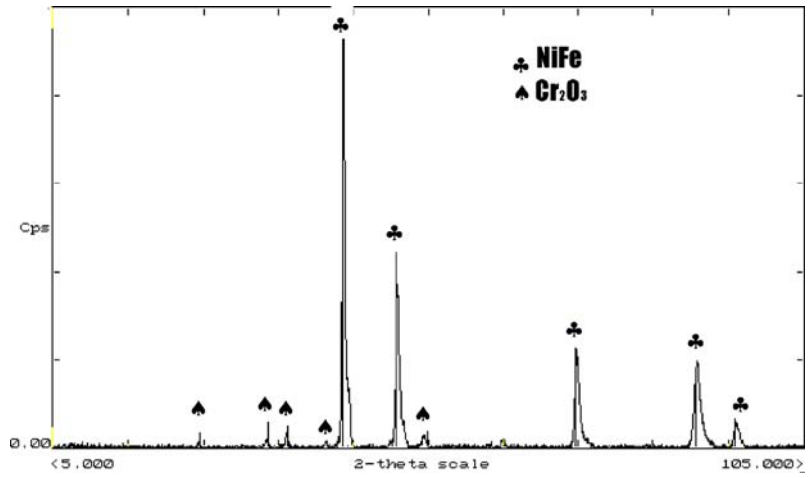

Fig. 4 XRD of A-625 as sprayed

Table 4 Tribological and microhardness results

	K_{ab}, mm^3/Nm	μ, 25 °C	$HV_{300\ g}$
A-625	1.02×10^{-4}	0.682	284 ± 32
B-625	1.10×10^{-4}	0.613	285 ± 08

Table 5 Loss of thickness after E-C test

	Loss of thickness, μm
A-625	5.9
B-625	35.8

boundaries that do not have any protective role under chloride environment (Ref 13). The chromium oxide is attacked by chloride salts in an oxidation atmosphere. This powder coating has a low thickness and shows discontinuities on the upper layers of the coating. However, the structure of the coating is also compact and homogeneous. The coatings are thick to assure a safety range for the tube protection. There are slight differences between the thicknesses of different coatings that are around 300 μm. The values of E-C and in situ tests are given in μm of thickness, to avoid these differences of the total coating thickness.

Porosity determined by image analysis is lower than 1.5% in both cases. X-ray diffraction of the sprayed material shows the presence of Cr_2O_3 in both cases, as shown in the spectra of Inconel wire in Fig. 4.

3.2 Results of Coating Characterization

Table 4 shows values of K_{ab}, abrasion coefficient from the Rubber-Wheel test (ASTM G65-91 D) at 50 N and results of μ (25 °C), the friction coefficient, under the Ball-on-Disk wear friction test at 5 N and 25 °C (ASTM G99-90) for HVT Inconel wire and DJH Inconel powder.

As can be seen, the values of the abrasion coefficient are very similar in both coatings. This means that the different morphologies of the feedstock material had no influence on the abrasion resistance if the appropriate spray conditions were used. HVT Inconel wire shows a

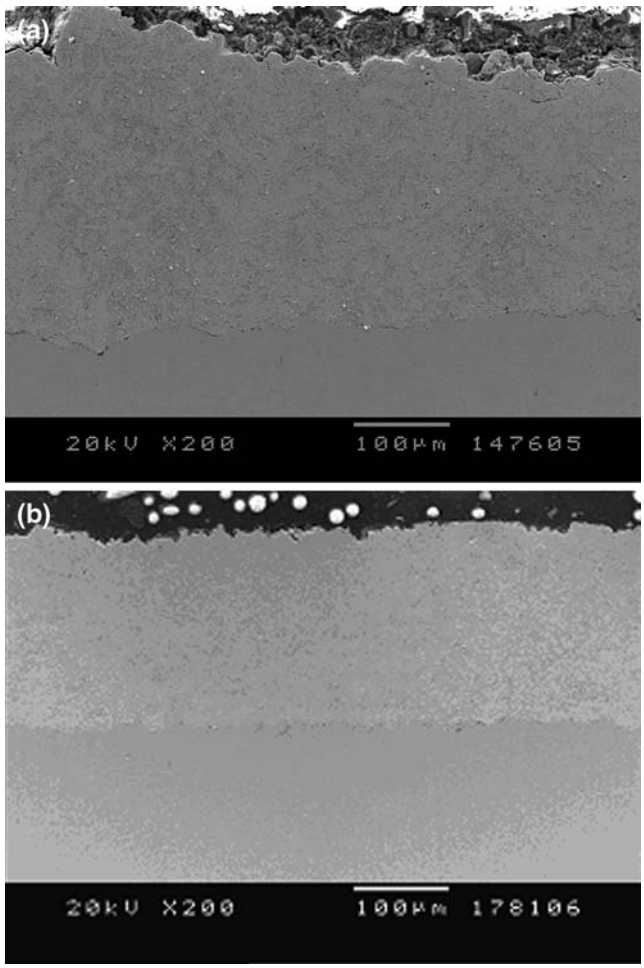

Fig. 5 (a) SEM structure of A-625 after E-C test and (b) SEM structure of B-625 after E-C test

higher friction coefficient, but it is very close to DJH Inconel powder values. Vickers microhardness of both alloys is also shown in Table 4.

It can be seen from all these results that no significant differences were observed in tribological properties. Similar resistance behavior under the erosion mechanisms of these tests can be expected. Tribological properties of these coatings are important due to the erosion processes produced by the flue gas.

The results of the E-C test is summarized in Table 5 as a loss of thickness of both alloys after 12 h. The values are given in μm of thickness, as well in the in situ test, to avoid the differences of the total coatings thickness.

Figure 5(a) and (b) shows structures of both alloys after the E-C test. Studying the micrographics, it can be concluded that E-C processes do not penetrate inside the coatings. Coatings A and B have good E-C resistances. Wire coating shows a better resistance under the E-C test, and this can be explained by the more continuous structure of the wire coating, which gives a higher erosion resistance. This compact structure of HVOF coatings deters the impacts of the hot salt solution that could deplete the coating if it has interconnected porosity (Ref 14).

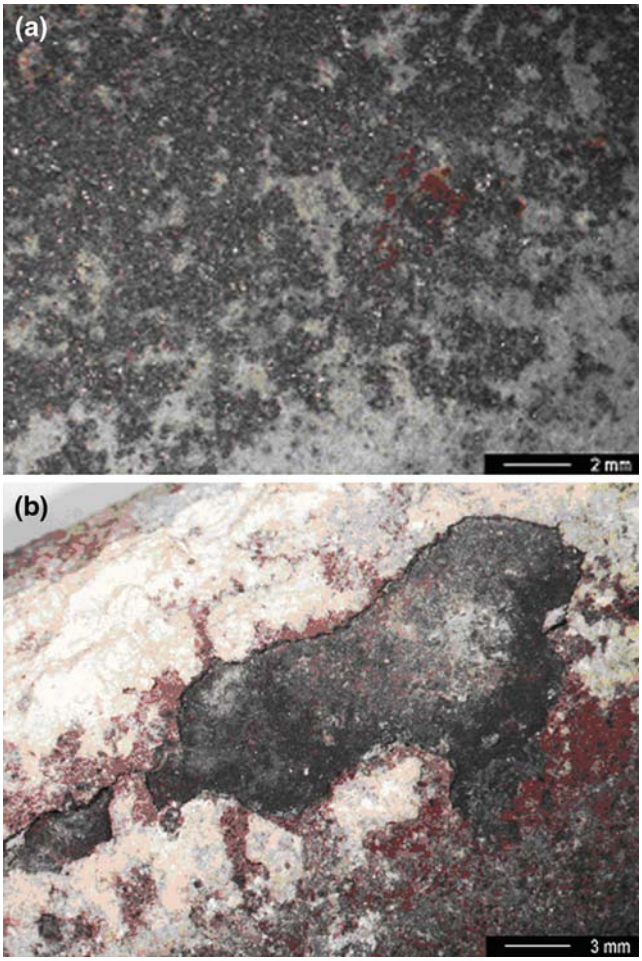

Fig. 6 (a) Image of the tube surface after 1 year in service and (b) image of an Fe-based coating surface after 1 year in service

Loss of thickness takes place through a depletion process that is typical in thermal spray coatings.

Electrolyte penetration through active zones such as interconnected porosity can oxidize internal zones of the coating. Due to the formation of porous phases like iron oxides or chromates, the material expansion initiates the depletion of the coating, producing loss of thickness. On the surface of the coating, the oxide layers were combined with high proportions of Cr and Ni to form Cr_2O_3 and NiO

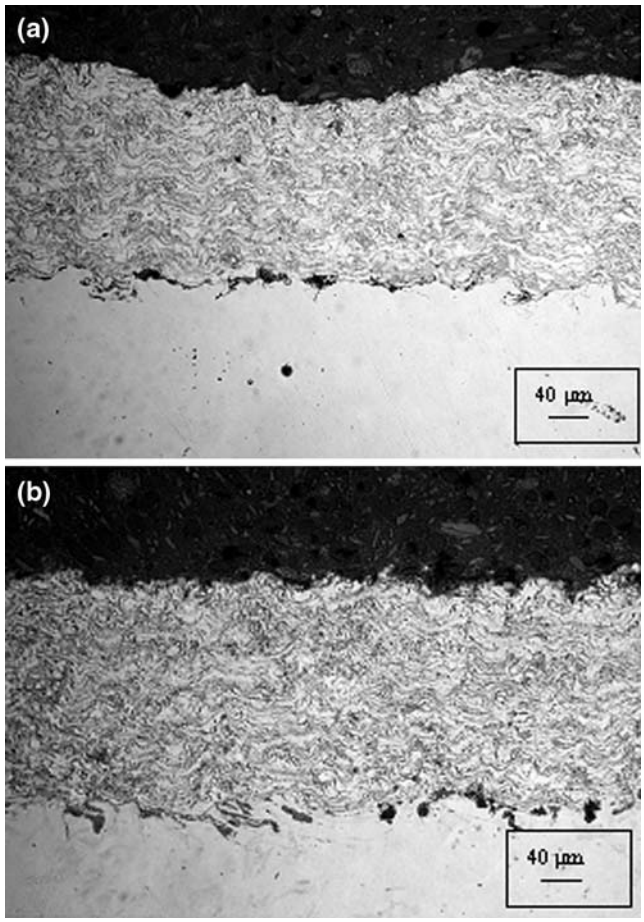

Fig. 7 (a) Frontal cross section of tube and (b) lateral cross section of tube

Table 6 Evaluation of thickness for the in situ test

	Thickness, μm
Original	164.2 ± 9.8
Corrosion zone	147.2 ± 11.2
E-C zone	155.2 ± 7.2

Table 7 Results of EDS analysis

Ni	O	Al	Nb	Mo
18.97	45.66	0.32	3.12	3.20

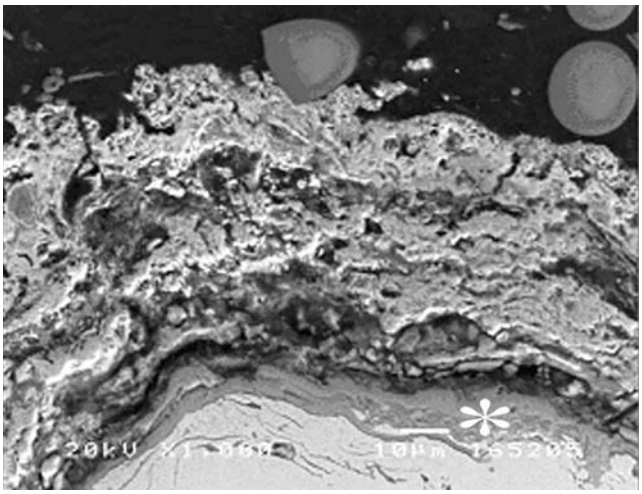

Fig. 8 Detail of coating cross section after 1 year in service and the point of the EDS analysis

(Ref 15, 16). A low amount of Mo and Nb was also detected. The results of this test lead to useing the wire coating on the in situ test.

3.3 In Situ Test

Inconel wire, which shows a better behavior on laboratory tests, was tested inside the boiler for 1 year of full service in the incinerator plant. The loss of thickness after this time was also unappreciable. Figure 6(a) shows the surface of the coated pipe after testing, where a continuous surface without corrosion processes can be seen and compared with the surface of the tube coated with an Fe-based alloy shown in Fig. 6(b). Fe-based coating tested under the same conditions shows discontinuities on the surface produced by the corrosion attack.

Figure 7(a) and (b) shows two different zones of the tube after testing. It can be appreciated that the corrosion frontal zone and the erosion lateral zone do not suffer erosion or corrosion attack.

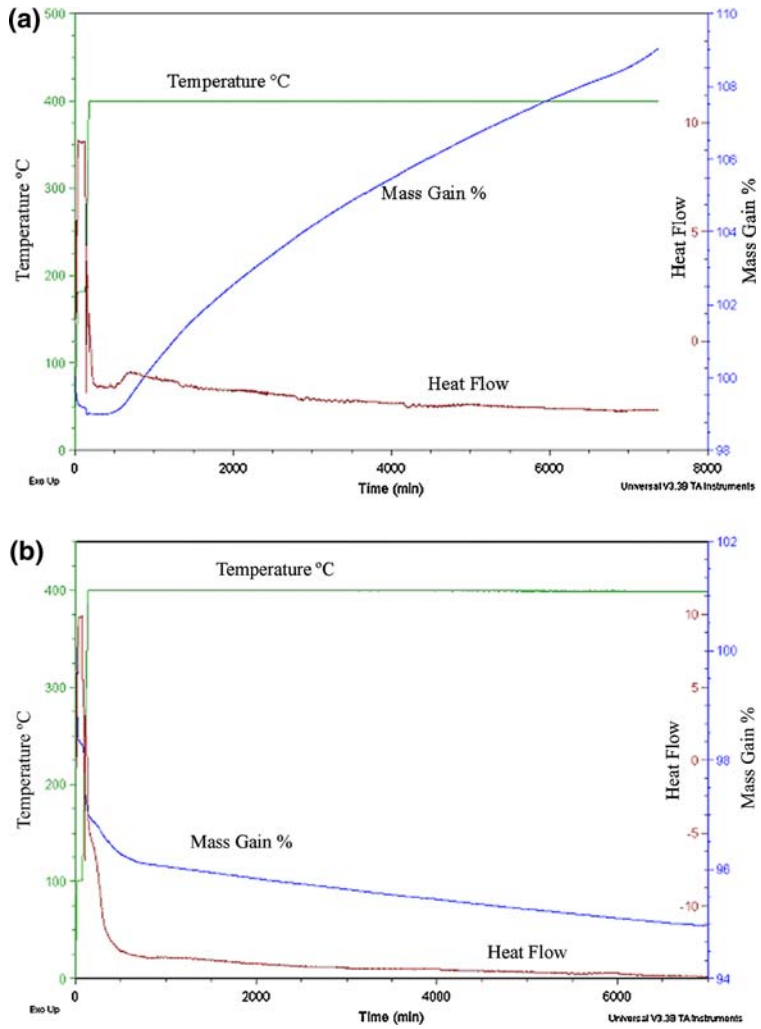

Fig. 9 (a) Profile of mass gain, temperature, and heat flow of uncoated tube steel under TGA test and (b) profile of mass gain, temperature, and heat flow of the Ni-based HVOF coating under TGA test

Results of the loss of thickness after 1 year of service are shown in Table 6. Two different attack zones were differentiated: the corrosion zone, where there is a perpendicular impact of the flue gas; and the E-C zone, which was on the lateral side of the tubes, where the abrasion mechanisms are favored (Ref 17). Mechanical and tribological coating properties are important for the coating resistance on the erosion zone. However, corrosion processes are more aggressive than erosion processes. The in situ loss of metal was so much lower than the measured one in the E-C tests because the laboratory test is so much aggressive and accelerates due to the salt concentration and continued attack focused on one point of the coating surface. The E-C test had been designed to reproduce the processes that takes place inside the MSWI in an accelerated way.

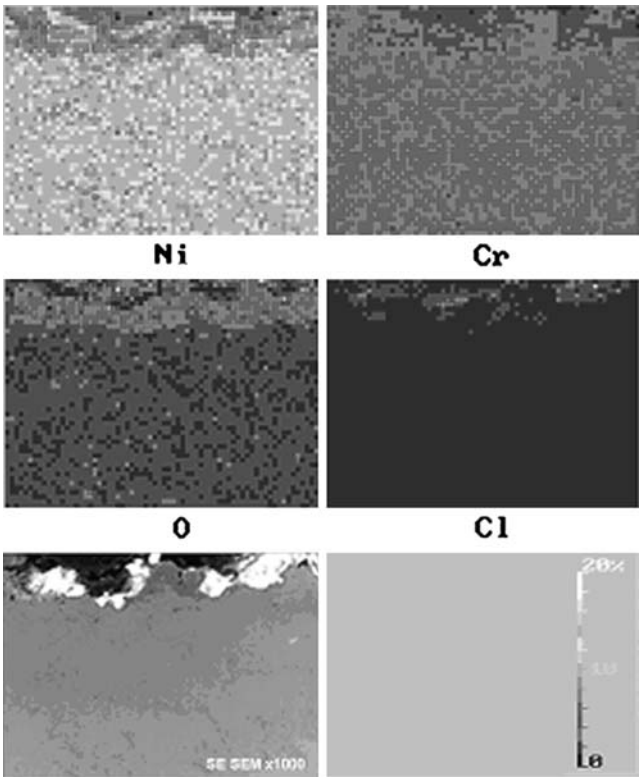

Fig. 10 EDS maps of major element concentration

In the MSWI where the test has been done, the average corrosion loss of thickness of the uncoated steel superheater tubes was around 120 μm a year. On the coated tubes it was only around 17 μm a year.

Table 7 shows the EDS analysis of the compact layer, which is marked on Fig. 8 also, rich in Ni, Cr, Mo, and Nb, with a high amount of oxygen. This phase, characterized as oxides mixture, delays the penetration of chlorides and the oxidation of the internal coating layers. The chromium amount in the corrosion product is higher than that in the as-sprayed coating. The oxidation of chromium is easier than the nickel oxidation, and in the face of chloride attack the chromium oxide is brittle and vulnerable and its production advances to deeper layers.

Figure 8 shows a detail of the compact oxide on the outer surface. A non-protective and porous layer can also be seen above the protection layer. The average partial pressure of Cl_2 inside the boiler is $p[Cl_2] = 10^{-7}$ bar (Ref 18). The presence of Cr_2O_3 and NiO can be expected with this atmosphere containing 5-10%O_2 in volume (Ref 19) Chromium oxide can form a continuous layer but is vulnerable to the chloride attacks; nickel oxide has good resistance but it does not have a passivation role (Ref 20).

Thermogravimetric tests show the difference produced on the oxidation resistance caused by HVOF coating. Figure 9(a) shows the gain of mass of the bare steel (AISI C-1055) pipe not covered. The mass increases 11% due to the formation of Fe_2O_3 (Ref 21, 22). Figure 9(b) shows that the coated sample mass instead of growing, decreases due to the evaporation of the molten chloride salts (Ref 23). This salt mixture is not volatile at this temperature, but

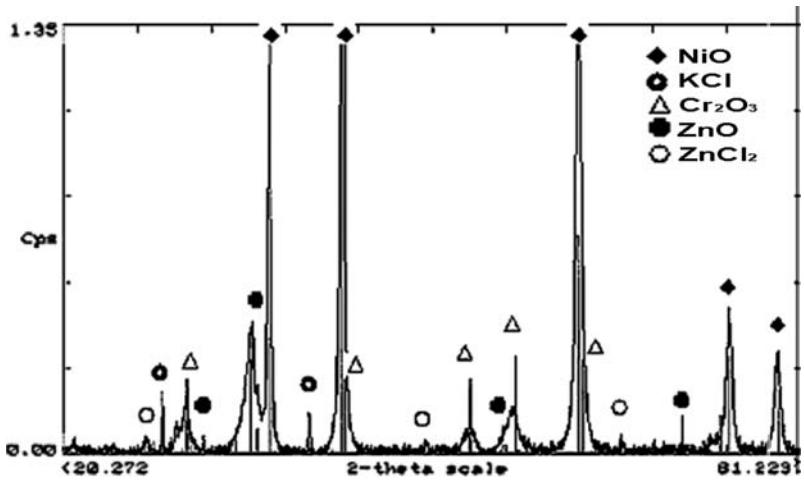

Fig. 11 XRD of the corrosion products for the static corrosion test

there was an air flow that kept the partial pressure of the salts very low. Under these conditions and during the 120 h of testing, there was some volatilization of salt mixture.

It can be seen that the difference between the two samples is very important and the coating improves the resistance under atmospheric oxidation conditions.

The EDS map in Fig. 10 shows the penetration of the oxygen and chloride after this 120 h as well as the nickel and chromium distribution.

3.4 Static Corrosion Test

Static corrosion testing on bulk materials was evaluated through XRD. Figure 11 shows the spectra of the bulk material after 360 h under salt mixture at 400 °C.

After all the tests were completed, the Ni alloy coating is seen to be a good protector of the exchanger tubes. Resistance under corrosion agents is due to the resistance of Ni under the chloride environment at elevated temperatures. The amount of Mo increases the corrosion resistance of the Ni-based alloys, which show a good corrosion resistance under chlorine-oxidizing atmospheres. Ni and Cr oxides are produced and can be detected by XRD. The EDS analyses detect the presence of Ni and Cr on the oxidized surface of the sample as non-protective oxide layers.

4. Conclusions

- Wire and powder HVOF coatings show good properties to protect steel exchanger pipes against the erosion produced by the impact of the ashes in the flue gas.
- No differences in tribological properties were found for Inconel wire coating or Inconel powder coating.
- The composition of the Ni alloy used in this work sprayed during different HVOF conditions shows good resistance against the corrosion process on the in situ tests and in the laboratory E-C test.
- XRD spectra show the presence of Ni and Cr oxides that can delay the attack of the Ni alloy by chlorides, but it does not have a passivation role.
- The better behavior of Inconel wire by HVT in comparison with Inconel powder by DJH on the laboratory E-C test is only justified by the better structure of wire coating that is more compact and avoids the penetration of the chlorides mixture.

Acknowledgments

M. Torrell would like to thank the Thermal Spray Center (University of Barcelona), as well as the *Generalitat de Catalunya* for project 2005 DSGR 00310 and the *Ministerio de Educación y Ciencia* for project MAT2000-0418-P4-03. The authors would especially like to acknowledge T.M. Comas S.A. for the spraying processes and the incineration plant SIRUSA for their collaboration in this work.

References

1. J.M. Guilemany, J. Nutting, and V. Sobolev, High Velocity Oxy Fuel Spraying. Theory, Structure-property Relationships and Applications. Maney Publishing, Leeds, UK, 2004
2. *ASM Handbook V13B Corrosion: Materials*, 2000 (Ohio), Materials Information Society, p 428-441. ISBN 0-87170-707-1
3. W.-M. Zhao, Y. Wang, L.-X. Dong, K.-Y. Wu, and J. Xue, Corrosion Mechanisms of NiCrBSi Coatings Deposited by HVOF, *Surf. Coat. Technol.*, 2005, **190**(2-3), p 293-298
4. T.S. Sidhu, S. Prakash, and R.D. Agrawal, Hot Corrosion of Some Superalloys and Role of High Velocity Oxy Fuel Spray Coatings a Review, *Surf. Coat. Technol.*, 2005, **198**(1-3), p 441-446
5. T.S. Sidhu, S. Parkash, and R.D. Agrawal, Characterisation of HVOF Sprayed NiCrBSi Coatings on NiS and Fe-Based Superalloys and Evaluation of Cyclic Oxidation Behaviour of Some Ni-Based Superalloys in Molten Salt Environment, *Thin Solid Films*, 2006, **515**, p 95-105
6. M.A. Uusitlao, P.M.J. Vuoristo, and T.A. Mäntylä, High Temperature Corrosion of Coatings and Boiler Steel in Oxidizing Chlorine-Containing Atmosphere, *Mater. Sci. Eng. A: Struct.*, 2003, **346**, p 168-177
7. M.A. Uusitlao, P.M.J. Vuoristo, and T.A. Mäntylä, High Temperature Corrosion of Coatings and Boiler Steels Below Chlorine-Containing Salt Deposits, *Corros. Sci.*, 2004, **46**, p 1311-1331
8. H.P. Nielsen, F.J. Frandsen, K. Dam-Johansen, and L.L. Baxter, The Implications of Chlorine-Associated Corrosion on the Operation of Biomass-Fired Boilers, *Prog. Energ. Combust.*, 2000, **26**, p 283-298
9. S. Zhao, X. Xie, and G.D. Smith, The Oxidation Behaviour of the New Nickel-Based Superalloy Inconel 740 With and Without Na_2SO_4, *Surf. Coat. Technol.*, 2004, **185**, p 178-183
10. Y.S. Li, Y. Niu, and W.T. Wu, Accelerated Corrosion of Pure Fe, Ni, Cr and Several Fe-Based Alloys Induced by $ZnCl_2$-KCl at 450 °C in oxidizing environment, *Mater. Sci. Eng. A: Struct.*, 2003, **345**, p 64-71
11. S.H. Lee, N.J. Themelis, and M.J. Castaldi, High Temperature Corrosion in Waste-to-Energy Boilers, *J. Therm. Spray Technol.*, 2007, **V16**(3), p 104-110
12. Y.S. Li and M. Spiegel, Models Describing the Degradation of FeAl and NiAl Alloys Induced by $ZnCl_2$-KCl Melt at 400-450°, *Corr. Sci.*, 2004, **46**(8), p 2009-2023
13. D. Zhang, S.J. Harris, and D.G. Mc Cartney, Microstructure Formation and Corrosion Behaviour in HVOF-Sprayed Inconel 625 Coating, *Mater. Sci. Eng. A: Struct.*, 2003, **344**, p 45-56
14. N. Kaharaman and B. Gülenç, Abrasive Wear Behaviour of Powder Flame Sprayed Coating on Steel Substrates, *Mater. Des.*, 2002, **23**, p 721-725
15. H.S. Sidhu, B.S. Sidhu, and S. Prakash, Hot Corrosion Behaviour of HVOF Sprayed Coatings on ASTM SA213-T11 Steel, *J. Therm. Spray Technol.*, 2007, **V16**(3), p 349-354
16. T.S. Sidhu, S. Prakash, and R.D. Agrawal, Hot Corrosion Studies of HVOF Sprayed Cr3C2-NiCr and Ni-20Cr coatings on Nickel-Based Superalloy at 900 °C, *Surf. Coat. Technol.*, 2006, **201**, p 792-800
17. J.M. Guilemany, M. Torrell, and J.R. Miguel, Comparison of Erosion-Corrosion Properties for Waste Incinerator Protection by HVOF Coatings. *Proceedings of Eurojoin 2006*, V1 (2006) p 173-182. European Federation of Welding. EWF Eurojoin 2006. Santiago de Compostela, Spain, 2006
18. K. Salmenoja, *Field and Laboratory Studies on Chlorine-Induced Corrosion in Boilers Fired with Biofuels*. Academic Dissertation, Abo Akadei, 2000, p 102
19. A. Zhas, M. Spigel, and H.J. Grabke, Chloridation and Oxidation of Iron, Chromium Nickel and Their Alloys in Chloridizing and Oxidizing Atmospheres at 400-700 °C, *Corr. Sci.*, 2000, **42**, p 1063-1122

20. M.A. Uusitalo, P.M.J. Vuoristo, and T.A. Mäntylä, High Temperature Corrosion of Coatings and Boiler Steel in Reducing Chlorine-Containing Atmosphere, *Surf. Coat. Technol.*, 2002, **V161**(2-3), p 275-285
21. H.J. Grabke, E. Reese, and M. Spiegel, The Effects of Chlorides, Hydrogen Chloride, and Sulfur Dioxide in the Oxidation of Steels below deposits, *Corr. Sci.*, 1995, **V37**(7), p 1023-1043
22. B.S. Sidhu and S. Parkash., Nickel Chromium Plasma Spray Coatings: A Way to Enhance Degradation Resistance of Boiler Tube Steel in Boiler Environment, *J. Therm. Spray Technol.*, 2006, **V151**(1), p 131-140
23. A. Ruh and M. Spiegel, Thermodynamic and Kinetic Consideration on the Corrosion of Fe, Ni and Cr Beneath a Molten KCl-$ZnCl_2$ mixture, *Corros. Sci.*, 2006, **48**, p 679-695